Shot-Noise-Limited Nanomechanical Detection and Radiation Pressure Backaction from an Electron Beam

S. Pairis, F. Donatini, M. Hocevar, D. Tumanov, N. Vaish, J. Claudon, Jean-Philippe Poizat, P. Verlot

Shot-Noise-Limited Nanomechanical Detection and Radiation Pressure Backaction from an Electron Beam

S. Pairis,[1] F. Donatini,[1] M. Hocevar,[1,2] D. Tumanov,[1,2] N. Vaish,[1,2] J. Claudon,[3] J.-P. Poizat,[1,2] and P. Verlot[4,*]
[1]Université Grenoble Alpes, CNRS, Grenoble INP, Institut Néel, F-38000 Grenoble, France
[2]CNRS, Inst. NEEL, "Nanophysique et semiconducteurs" group, 38000 Grenoble, France
[3]Univ. Grenoble Alpes, CEA, INAC, PHELIQS, "Nanophysique et semiconducteurs" group, F-38000 Grenoble, France
[4]School of Physics and Astronomy, University of Nottingham, Nottingham, NG7 2RD, United Kingdom

(Received 6 February 2018; revised manuscript received 16 September 2018; published 1 March 2019)

Detecting nanomechanical motion has become an important challenge in science and technology. Recently, electromechanical coupling to focused electron beams has emerged as a promising method adapted to ultralow scale systems. However the fundamental measurement processes associated with such complex interaction remain to be explored. Here we report a highly sensitive detection of the Brownian motion of μm-long semiconductor nanowires (InAs). The measurement imprecision is found to be set by the shot noise of the secondary electrons generated along the electromechanical interaction. By carefully analyzing the nanoelectromechanical dynamics, we demonstrate the existence of a radial backaction process that we identify as originating from the momentum exchange between the electron beam and the nanomechanical device, which is also known as radiation pressure.

DOI: 10.1103/PhysRevLett.122.083603

Introduction.—Nanomechanical devices are raising increasing interest both in science and technology [1] and are spreading in various fundamental and applied fields [2–6]. Recently, electromechanical coupling to focused electron beams has been pointed out as a very promising alternative to optical schemes for nanomechanical systems with dimensions well below the diffraction limit [7,8], opening unprecedented technological perspectives such as using nanotubes as scanning probe sensors [9], atomically controlled *e*-beam assisted deposition [10] and 3D nanoprinting [11]. In this context, where focused electron beams are used both as detection and control tools, it becomes crucial to identify and characterize electromechanical backaction mechanisms that ultimately limit the accuracy and potential of these applications. Importantly, this question has not yet been thoroughly explored in the relevant context of massive fermion-based dissipative measurements, which therefore remains opened. Recently, some of us have reported results deep in the electrothermal regime [7]. Such effects however remain strongly dependent upon structural anisotropies [12] and therefore do not represent a fundamental backaction limitation within the electromechanical measurement process. Moreover, the origin of the measurement imprecision within such a strongly dissipative process, where the incident probe is practically annihilated during the interaction, remains to be addressed, previous investigations being essentially limited by technical noises [7,8].

In this Letter, we experimentally investigate the basic physical processes (i.e., measurement noise and measurement backaction [13]) associated with the electromechanical coupling between a focused electron beam and a nanomechanical resonator. We report ultrasensitive detection of the Brownian motion of μm-long InAs nanowires, with a sensitivity that can be as low as $S_{xx}^{\mathrm{imp}} = (270\ \mathrm{fm}/\sqrt{\mathrm{Hz}})^2$, comparable or even better than state-of-the-art cavityless optomechanical readout schemes for equivalent probe powers [14]. We demonstrate that the sensitivity is set by the gradient of secondary electron emission, with an imprecision originating from the shot noise of the emitted secondary electrons. In contrast to a previous work [7], our nanomechanical system is found to be weakly sensitive to dissipative electrothermal gradients. Combined with the geometry of our experiment, this property enables us to extract the fundamental component of the measurement backaction process and demonstrate the existence of a radial force associated with the nanoelectromechanical measurement, which we identify as the radiation pressure force exerted by the electron beam on our nanomechanical structure. In a more general perspective, our work and methods show that motion correlations between the two orthogonal modes of a two-dimensional resonator enable us to reveal sensitive information on the origin of the measurement backaction force, which may be further extended to various physical contexts such as light momentum measurements [15,16] and ultrasensitive force microscopy [17,18].

Experimental setup.—The nanomechanical systems investigated in this Letter consist of as-grown InAs nanowires. We grew the nanowires perpendicularly on a (111)B InAs substrate by the vapor solid liquid method using 50 nm-gold catalysts in a molecular beam epitaxy setup.

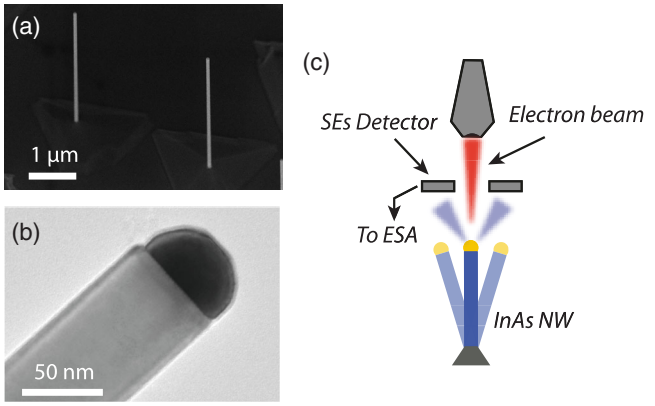

FIG. 1. (a) Scanning electron micrograph showing two InAs nanowires similar to those used in this work (≃25° tilted view). (b) Transmission electron microscopy image of the upper part of a InAs nanowire. The dark hemisphere at the top of the nanowire is the gold catalyst. (c) Schematic depicting the principle of the experiment. A focused electron beam is sent on the nanowire, whose vibrations result in fluctuations of the secondary electron (SE) current. These fluctuations are monitored using a secondary electrons detector which is further connected to an electrical spectrum analyzer (ESA).

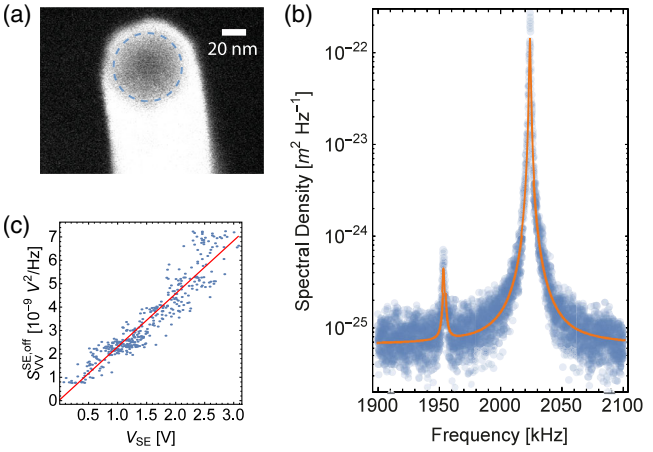

FIG. 2. (a) Magnified scanning electron micrograph showing an InAs NW similar to those used in this Letter (top view). The dashed line emphasizes the detection annulus, that is the region where the e-beam spot is positioned for measuring nanomechanical motion (see text). (b) Electromechanical fluctuations spectrum obtained with NW_1. The experimental data (dots) are fitted using a double Lorentzian model (solid line). (c) Evolution of the measurement noise background $S_{VV}^{SE,off}$ as a function of the average secondary electrons detector output V_{SE}. The red, solid line corresponds to a linear model, characteristic of Poisson statistics.

Representative structures are shown in Figs. 1(a) and 1(b). The resulting nanowires are surmounted by a hemispherical gold droplet [see Fig. 1(b)] and feature a wurtzite crystal structure with a limited number of stacking faults. The nanowires have lengths and diameters typically ranging from 4 μm–5.5 μm and 60 nm–80 nm, respectively. The results hereby reported have been obtained using three distinct samples referenced as $NW_{j\in\{1,2,3\}}$ in the following. The samples are mounted in a field emission scanning electron microscope operating with a probe current set to $I_p = 186$ pA and an acceleration voltage $V = 3$ kV. The 3D positioning stage hosting the sample is subsequently carefully aligned for matching the electron beam direction to the axis of the nanowires. Measuring the defocusing between the wafer plane and the edge of the nanowires enables us to estimate a residual tilt angle $\alpha \simeq 2.4°$. Figure 2(a) shows a typical scanning electron micrograph obtained in such conditions with our samples.

The nanomechanical motion of the nanowire is detected by setting the electron beam spot to a high-contrast region of the tip surface, on the external annulus delimiting the central, dark region [which will be recalled as "detection annulus" in the following, see Fig. 2(a)]. The vibrations of the nanowire result in fluctuations of the secondary electrons (SEs) current, which are directly monitored by connecting a low noise electrical spectrum analyzer to the amplified SEs detector output [7,8] [see Fig. 1(c)]. The electromechanical spectrum obtained with NW_1 is shown in Fig. 2(b). Two peaks are revealed, corresponding to each of the two vibrational directions of the nanowire. Remarkably, the highest noise peak is resolved with a signal-to-noise ratio exceeding 30 dB despite the relatively high mechanical frequency. To calibrate the electromechanical fluctuation spectrum, we assume the nanomechanical noise to be thermally driven—this hypothesis will be further confirmed—with an effective mass $m_1 = 22$ fg determined from the sample geometry, mechanical resonance frequency $\Omega_1/2\pi = 2023.9$ kHz, and temperature $T \simeq 300$ K. The SEs fluctuations are subsequently converted into equivalent displacement by matching the SEs' current variance with the thermal noise variance $(\Delta x_{th,1})^2 = (k_B T)/(m_1 \Omega_1^2)$. In particular, we find a displacement sensitivity $S_{xx}^{imp} \simeq (270\ \text{fm}/\sqrt{\text{Hz}})^2$, which even exceeds the performances of the most sensitive optical cavityless detection schemes for freestanding resonators with comparable dimensions [14]. The origin of the detection background is determined by measuring the evolution of the off-resonant spectral density of the SEs current $S_{II}^{SE,off}$ as a function of the average scattered current $\bar{I}_{SE}$. We find a linear relationship, $S_{II}^{SE,off} \propto \bar{I}_{SE}$, characteristic of a Poisson statistics, which demonstrates that SEs' electromechanical detection is shot noise limited [see Fig. 2(c)]. We however emphasize that the underlying mechanism is very different from the one usually encountered, e.g., in dispersive optomechanical detection schemes, whose measurement noise properties essentially rely on the input probe state. Here, because of the strongly dissipative nature of the electromechanical interaction, the input beam is almost entirely destroyed, and the measured fluctuations essentially reflect the discrete nature of the secondary electrons.

Two-dimensional measurement and sensitivity.—To further address the behavior of the electromechanical coupling, we acquire the SE's fluctuation spectra while browsing the e-beam spot position all around the edge of the dark central disk. Since we are detecting variations of the SE's emission rate, the corresponding intensity fluctuations δI_{SE} can be generally written as:

$$\delta I_{\mathrm{SE}}(\mathbf{r_0}, t) \simeq \nabla \bar{I}_{\mathrm{SE}}(\mathbf{r_0}) \cdot \delta\mathbf{r}(t), \tag{1}$$

with $\nabla \bar{I}_{\mathrm{SE}}$ the SEs intensity gradient, $\mathbf{r_0}$ the average, two-dimensional position of the nanowire's tip in the horizontal plane and $\delta\mathbf{r}(t)$ the time dependent position variations, $\delta\mathbf{r}(t) = \delta x_1(t)\mathbf{e_1} + \delta x_2(t)\mathbf{e_2}$ ($\mathbf{e_{1,2}}$ as the eigendirections of vibration and $\delta x_{1,2}(t)$ as the associated displacements fluctuations). Because of the rotational symmetry [see Fig. 2(a)], the intensity gradient is radial, $\nabla \bar{I}_{\mathrm{SE}} = [\partial \bar{I}_{\mathrm{SE}}/\partial r]_{\mathbf{r_0}} \mathbf{e_r}$ where ($\mathbf{e_r}$, $\mathbf{e_\theta}$ is the polar base defined as $\mathbf{e_r} = \cos\theta\mathbf{e_1} + \sin\theta\mathbf{e_2}$ and $\mathbf{e_\theta} = -\sin\theta\mathbf{e_1} + \cos\theta\mathbf{e_2}$). The SEs intensity fluctuations therefore reflect the combination of both displacements $\delta x_1(t)$ and $\delta x_2(t)$, weighted by their projection on the intensity gradient, $\delta I_{\mathrm{SE}}(\mathbf{r_0}, t) = [\partial \bar{I}_{\mathrm{SE}}/\partial r]_{\mathbf{r_0}} \times [\cos\theta\delta x_1(t) + \sin\theta\delta x_2(t)]$, from which the expression of the electromechanical fluctuations spectrum [defined, in the limit of stationary fluctuations as $S_{\mathrm{II}}^{\mathrm{SE}}[\mathbf{r_0}, \Omega] = \int_{-\infty}^{+\infty} dt e^{-i\Omega t}\langle \delta I_{\mathrm{SE}}(\mathbf{r_0}, 0)\delta I_{\mathrm{SE}}(\mathbf{r_0}, t)\rangle$, can be inferred:

$$S_{\mathrm{II}}^{\mathrm{SE}}[\mathbf{r_0}, \Omega] = \left(\frac{\partial \bar{I}_{\mathrm{SE}}}{\partial r}\right)_{\mathbf{r_0}}^2 \times (\cos^2\theta S_{\mathrm{xx},1}^{r_0,\theta}[\Omega] + \sin^2\theta S_{\mathrm{xx},2}^{r_0,\theta}[\Omega] + \sin 2\theta \mathrm{Re}\{\langle \delta x_1[\Omega]\delta x_2[-\Omega]\rangle_{r_0,\theta}\}) \tag{2}$$

with Ω as the Fourier frequency, and $S_{\mathrm{xx},1}^{r_0,\theta}$ (resp. $S_{\mathrm{xx},2}^{r_0,\theta}$) as the displacement fluctuations spectrum associated with δx_1 (resp. δx_2). Note that the superscript r_0, θ is to remind that the motion spectral density includes the contribution of a measurement backaction *a priori*, which depends on the electromechanical coupling rate, and henceforth on the polar coordinates. The second line of Eq. (2) represents θ-dependent motion correlations between the two vibrational directions, which occur in presence of a common external driving source [19], resulting in strong spectral distortions compared to the uncorrelated bi-Lorentzian model [first line of Eq. (2)].

Figure 3(a) shows four electromechanical spectra acquired at four distinct azimuths (data acquired with NW_2). The experimental data (dots) are fitted using a standard uncorrelated bi-Lorentzian model (solid lines, with $S_{\mathrm{xx},j}^{r_0,\theta}[\Omega] = S_{\mathrm{FF},j}^{r_0,\theta}/m_j^2((\Omega_j^2 - \Omega^2)^2 + \Gamma_j^2\Omega^2)$, $S_{\mathrm{FF},j}^{r_0,\theta}$ the white force spectral density driving nanomechanical motion in direction and Γ_j the mechanical damping rate associated to mode j). Since no deviation from this model was observed for any azimuth, we therefore conclude that the correlation term of Eq. (2) vanishes, $\langle \delta x_1[\Omega]\delta x_2[-\Omega]\rangle_\theta = 0$. We subsequently compute the ratio of the peak values $r^2[\theta] = \tan^2\theta \times S_{\mathrm{xx},2}^{r_0,\theta}[\Omega_2]/S_{\mathrm{xx},1}^{r_0,\theta}[\Omega_1]$ [see Fig. 3(b)]. The experimental data (dots) are adjusted using a $\tan^2$ model (dashed line), from which we deduce that $S_{\mathrm{xx},2}^{r_0,\theta}[\Omega_2] \simeq S_{\mathrm{xx},1}^{r_0,\theta}[\Omega_1]$, $\forall\,\theta$. Assuming equal effective masses in both vibrational directions, $m_2 = m_1 = m$, we conclude that $S_{\mathrm{FF},1}^{r_0,\theta} \simeq S_{\mathrm{FF},2}^{r_0,\theta}$, $\forall\,\theta$. This establishes thermal noise as the dominant random source of motion.

Backaction gradients.—To further investigate the backaction processes associated with the electromechanical

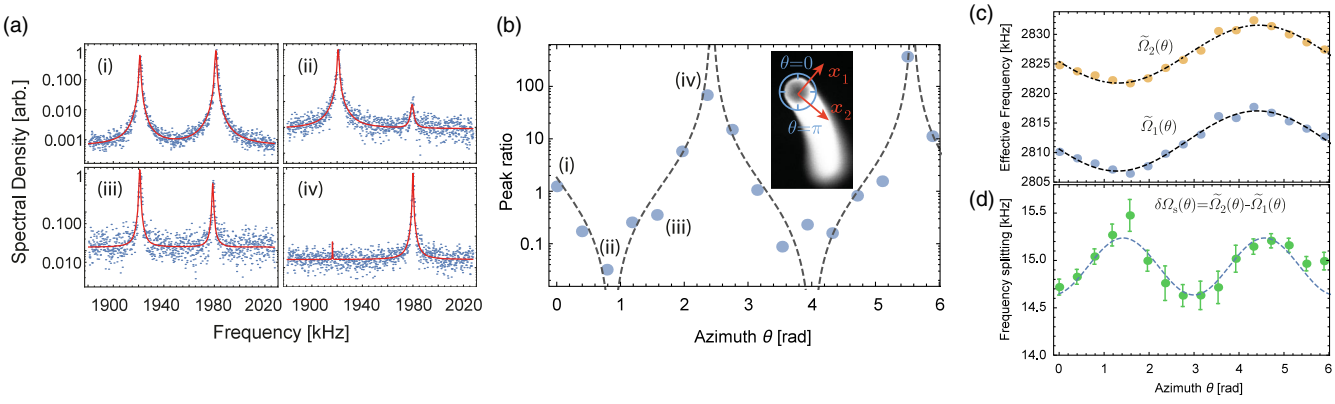

FIG. 3. (a) Four electromechanical fluctuation spectra acquired at four distinct azimuthal positions of the circumference of the nanowire NW_2 [$\theta = \pi/16, 3\pi/16, 5\pi/16$, and $7\pi/16$ from (i) to (iv), see Fig. 3(b) for conventions]. (b) Ratio of the spectral amplitudes of the two peaks as a function of the azimuth. The experimental data points (dots) are fitted using a tangent squared model (dashed line), whose asymptotes enable us to determine the direction of the eigenaxis of vibration. Inset: Scanning electron micrograph of the device showing the conventions used for the azimuth as well as the inferred direction of the vibrational axis. (c) Evolution of the effective mechanical resonance frequencies $\tilde{\Omega}_1$ and $\tilde{\Omega}_2$ as a function of the azimuth (data acquired with NW_3). Dashed lines are sinusoidal fit (see text). (d) Frequency splitting as a function of the azimuth (data acquired with NW_3). The experimental data (dots) are fitted using a π-periodic sinusoidal model, characteristic of the (radial) radiation pressure backaction force (see text).

measurement, we now examine the effects produced by their gradients, which generally leave much stronger dynamical signatures than fluctuations at room temperature (as, e.g., for dynamical backaction in optomechanics [16,20]). The backaction force is essentially the sum of two contributions of different nature, $\mathbf{F_{ba}} = \mathbf{F_d} + \mathbf{F_q}$. Here $\mathbf{F_d}$ denotes the contribution of dissipative mechanisms, which result from heating due to e-beam absorption. Previous work has shown that electrothermal actuation is the dominant dissipative mechanism with semiconducting nanomechanical devices [7]: a fraction of the electrical energy carried by the incident electron beam is released as heat, yielding to deformations that are equivalent to nanomechanical motion in one invariable direction (imposed by the imperfect geometry of the nanowire), $\mathbf{F_d}(r,\theta) = F_\mathrm{d}(r,\theta)\cos\theta_d \mathbf{e_1} + F_\mathrm{d}(r,\theta)\sin\theta_d \mathbf{e_2}$, with F_d as the modulus of the electrothermal force and θ_d as the direction of the force in the basis $(\mathbf{e_1}, \mathbf{e_2})$. In contrast, $\mathbf{F_q}$ denotes the measurement backaction force, resulting from the only action of measuring the system, independent from the experimental environment [13]. We attribute this force to radiation pressure whereby the incident electrons are transferring part of their momentum to the nanowire in the radial direction, $\mathbf{F_q}(r,\theta) = F_\mathrm{q}(r,\theta)\mathbf{e}_\mathrm{r}$, with F_q the modulus of the radiation pressure force.

Force gradients modify the effective restoring force in both nanomechanical motion directions, resulting in a frequency shift $\delta\Omega_j^k = 1/(2m\Omega_j)(\partial F_{k,j}/\partial x_j)$ $(k \in \{\mathrm{d},\mathrm{q}\}, j \in \{1,2\})$, with $F_{k,j} = \mathbf{F_k}\cdot\mathbf{e_j}$. Taking the above given general expression for $\mathbf{F_d}$ and $\mathbf{F_q}$ subsequently yields to the expressions given in the Supplemental Material [21].

In addition to the effects of backaction gradients, the mechanical resonance frequencies may be prominently affected by temperature-induced internal changes of the nanomechanical system [24,25], resulting in common mode frequency variations $\delta\Omega_1^\mathrm{th}(\theta) = \delta\Omega_2^\mathrm{th}(\theta) = \delta\Omega_\mathrm{th}(\theta) = \sum_k (\partial\Omega_0/\partial p_k)(\partial p_k/\partial T)\delta T(\theta)$, with δT the temperature variation and $p_k \in \{R_0, L, Y_\mathrm{InAs}, \rho_\mathrm{InAs}\}$ the kth parameter involved in the expression of the intrinsic mechanical resonance frequency $\Omega_0 \simeq [0.6\pi/L]^2\sqrt{(\pi Y_\mathrm{InAs}R_0^2)/(\rho_\mathrm{InAs})}$ (with R_0 the radius of the nanowire, Y_InAs Young's modulus and ρ_InAs the mass density). In total, each mechanical resonance frequency shift generally expresses as the sum of three terms, $\delta\Omega_i = \delta\Omega_i^\mathrm{d} + \delta\Omega_i^\mathrm{q} + \delta\Omega_\mathrm{th}$.

Figure 3(d) shows the evolution of the mechanical resonance frequencies $\tilde{\Omega}_i(\theta) = \Omega_i + \delta\Omega_i(\theta)$ of NW_3 as a function of the azimuth of the electron beam spot on the detection annulus (Ω_i the intrinsic mechanical resonance frequency associated with mode i). To zeroth order, both frequencies are shifting from similar, sinusoidal amounts (dot-dashed and dashed lines). Such behavior essentially reflects the contribution of temperature changes, $\delta\Omega_i(\theta) \simeq \delta\Omega_\mathrm{th}(\theta)$, since force gradients cannot generate identical $2\pi-$ periodic frequency shifts other than zero (see Supplemental Material [21]).

The sinusoidal evolution of the temperature is explained because of the small tilt angle α of the incident electron beam with respect to the top face of the nanowire, yielding to azimuth dependent energy deposition (see Supplemental Material [21]). At room temperature, the coefficient of thermal expansion of InAs is on the order of $\alpha_\mathrm{InAs} \simeq 4.5\times10^{-6}$ K^{-1} [26], negligible compared to the relative change of Young's modulus $(1/Y_\mathrm{InAs})(\partial Y_\mathrm{InAs}/\partial T) \simeq 1.2\times10^{-4}$ K^{-1} [27], yielding to $\delta\Omega_\mathrm{th}(\theta) \simeq [1/(2Y_\mathrm{InAs})](\partial Y_\mathrm{InAs}/\partial T)\Omega_0 \times \delta T(\theta)$. From the amplitude of the sine wave $\Delta\Omega_\mathrm{th}/2\pi = 5.15$ kHz, it is possible to determine the total temperature variation over scanning the detection annulus $\Delta T = 2\times 2Y_\mathrm{InAs}(\partial Y_\mathrm{InAs}/\partial T)^{-1}\times[\Delta\Omega_\mathrm{th}/\Omega_0] \simeq 58$ K, in reasonable agreement with simulations of energy absorption (see Supplemental Material [21]). In a more general perspective, this result exemplifies how our electromechanical approach enables us to perform thermal measurements *in situ*, and in particular to estimate e-beam induced heating in nanomechanical structures.

Radiation pressure contribution.—To complete our Letter, we examine the evolution of the frequency splitting $\delta\Omega_s(\theta) = \tilde{\Omega}_2(\theta) - \tilde{\Omega}_1(\theta)$, which enables us to reject the common-mode frequency variations as a function of the azimuth. Because of the nondegenerate nature of the nanowire, the splitting reads $\delta\Omega_s(\theta) = \delta\Omega_{s,0} + \{\delta\Omega_2^\mathrm{d}(\theta) - \delta\Omega_1^\mathrm{d}(\theta)\} + \{\delta\Omega_2^\mathrm{q}(\theta) - \delta\Omega_1^\mathrm{q}(\theta)\}$, with $\delta\Omega_{s,0}/2\pi \simeq 15.2$ kHz the bare fundamental resonance frequency splitting. From the above study of the thermal shifts, it is possible to show that dissipative backaction gradients do not contribute to the azimuthal variations of the frequency splitting (i.e., $\delta\Omega_2^\mathrm{d}(\theta) - \delta\Omega_1^\mathrm{d}(\theta)$ is θ independent, see Supplemental Material [21]). Any observed evolution is therefore necessarily attributed to the fundamental, radiation pressure component. Assuming rotational invariance $(\partial F_\mathrm{q}/\partial\theta = 0)$, the corresponding contribution can be further expressed as $2m\Omega_0\{\delta\Omega_2^\mathrm{q}(\theta) - \delta\Omega_1^\mathrm{q}(\theta)\} = [F_\mathrm{q}/R - (\partial F_\mathrm{q}/\partial r)_R]\cos 2\theta$, which is a π-periodic sinusoidal function of the azimuth, noticeably. Figure 3(d) shows the experimentally obtained azimuthal evolution of the frequency splitting (dots). The dashed line is an offset, π-periodic sine wave fit, in excellent agreement with our model.

Discussion.—To gain additional qualitative insight and relate the measured frequency splitting amplitude $\Delta\Omega_s/2\pi = 600$ Hz to the radiation pressure force, we further assume a quadratic form $F_\mathrm{q}(r) = \varphi_\mathrm{q}'' r^2$ [which can be justified by the curved secondary electron intensity profile, see Fig. 2(a)]. This enables us to estimate the amplitude of the radiation pressure force exerted in the horizontal plane, $F_\mathrm{q}(R) = m\Omega_0\Delta\Omega_s R \simeq 34$fN. An interpretation of this value can be drawn by considering the associated uncertainty product $\sqrt{S_\mathrm{xx}^\mathrm{imp}\times S_\mathrm{FF}^\mathrm{imp}}$, with

$\sqrt{S_{\mathrm{FF}}^{\mathrm{imp}}} = F_{\mathrm{q}}/\sqrt{I_{\mathrm{p}}/e} \simeq 9.8 \times 10^{-19}$ N/$\sqrt{\mathrm{Hz}}$ the radiation pressure backaction noise (I_{p}/e the incident electron flux, $e \simeq 1.6 \times 10^{-19}$ C the electron charge). We obtain $\sqrt{S_{\mathrm{xx}}^{\mathrm{imp}} \times S_{\mathrm{FF}}^{\mathrm{imp}}} \simeq 5300\hbar/2$. While being much reduced compared to previous studies [7], this result indicates that the present electromechanical measurements operate far from the Heisenberg limit, for which a product of $(\hbar/2)$ is expected. This excess of imprecision may arise from two contributions. First, it is likely that we operate far from the Cramér-Rao bound, which would correspond to the highest attainable displacement sensitivity [28]. Indeed for symmetry reasons, the present Letter has been achieved by operating on the detection annulus, which is at the expense of a decreased secondary electron gradient, yielding to a much reduced displacement sensitivity. The second reason that may explain the observed imprecision excess is more fundamental and related to the massive nature of the electrons. As demonstrated above, the measurement imprecision is set by secondary electron shot noise, which depends on the secondary electron yield (SEY), which is the number of emitted secondary electrons per incident primary electron. The SEY is a function of the incident electrons velocity, which is determined by the acceleration voltage. For gold, the SEY peaks around $V \simeq 300$ V [29], whereas we pump our systems using electrons that are more than three times faster ($V = 3$ keV), resulting in a backaction noise excess.

Conclusion.—In conclusion, we have reported ultrasensitive, shot-noise-limited nano-electromechanical detection of very high frequency semiconducting nanowires. Placing ourselves in a radial detection geometry, we have been able to show that this technique comes with negligible backaction noise at room temperature. The measurement backaction manifests as frequency changes. By analyzing the spectral behavior as a function of the electron beam spot azimuth in the upper horizontal plane, we have shown that it is possible to isolate the contribution of the radiation pressure force gradient as opposed to dissipative backaction mechanisms. Our results open the fundamental perspective to further explore the dissipative measurement regime with massive fermions. This regime has already attracted attention albeit with massless bosons (photons), e.g., with studies of the quantum limits of photothermal cooling [30]. Here, in contrast, the massive nature of the electrons enables us to somehow tune the backaction noise with respect to the measurement noise. How the fundamental measurement principles ultimately affect the corresponding sensitivity limits remains to be explored. In particular, the use of a material with much higher secondary electron yield, operated at much lower acceleration, may enable us to approach (or even beat) the Heisenberg limit.

We gratefully acknowledge M. Orú, D. Beznasiuk, E. Bellet-Amalric, and J.-M. Gérard for fruitful and stimulating discussions. This work is supported by The French National Research Agency (Projects No. NOFX2015 ANR-15-CE09-0016 and QDOT ANR-16-CE09-0010). P. V. acknowledges support from the ERC Starting Grant No. 758794 'Q-ROOT'.

*pierre.verlot@nottingham.ac.uk

[1] A. N. Cleland, *Foundations of Nanomechanics: From Solid-State Theory to Device Applications* (Springer Science & Business Media, Berlin; Heidelberg, Germany; New York, 2013).
[2] O. Arcizet, V. Jacques, A. Siria, P. Poncharal, P. Vincent, and S. Seidelin, Nat. Phys. **7**, 879 (2011).
[3] I. Yeo, P.-L. De Assis, A. Gloppe, E. Dupont-Ferrier, P. Verlot, N. S. Malik, E. Dupuy, J. Claudon, J.-M. Gérard, A. Auffèves *et al.*, Nat. Nanotechnol. **9**, 106 (2014).
[4] D. Rugar, R. Budakian, H. Mamin, and B. Chui, Nature (London) **430**, 329 (2004).
[5] J. Tamayo, P. M. Kosaka, J. J. Ruz, Á. San Paulo, and M. Calleja, Chem. Soc. Rev. **42**, 1287 (2013).
[6] J. Chaste, A. Eichler, J. Moser, G. Ceballos, R. Rurali, A. Bachtold, and S. Information, Nat. Nanotechnol. **7**, 301 (2012).
[7] A. Niguès, A. Siria, and P. Verlot, Nat. Commun. **6**, 8104 (2015).
[8] I. Tsioutsios, A. Tavernarakis, J. Osmond, P. Verlot, and A. Bachtold, Nano Lett. **17**, 1748 (2017).
[9] A. Siria and A. Niguès, Sci. Rep. **7**, 11595 (2017).
[10] A. Tavernarakis, A. Stavrinadis, A. Nowak, I. Tsioutsios, A. Bachtold, and P. Verlot, Nat. Commun. **9**, 662 (2018).
[11] J. Pablo-Navarro, D. Sanz-Hernández, C. Magén, A. Fernández-Pacheco, and J. M. de Teresa, J. Phys. D **50**, 18LT01 (2017).
[12] T. Ikuno, S.-i. Honda, T. Yasuda, K. Oura, M. Katayama, J. G. Lee, and H. Mori, Appl. Phys. Lett. **87**, 213104 (2005).
[13] V. B. Braginsky, F. Y. Khalili, and K. S. Thorne, *Quantum Measurement* (Cambridge University Press, Cambridge, England, 1995).
[14] J. M. Nichol, E. R. Hemesath, L. J. Lauhon, and R. Budakian, Appl. Phys. Lett. **93**, 193110 (2008).
[15] R. A. Beth, Phys. Rev. **50**, 115 (1936).
[16] T. J. Kippenberg and K. J. Vahala, Science **321**, 1172 (2008).
[17] L. M. de Lépinay, B. Pigeau, B. Besga, P. Vincent, P. Poncharal, and O. Arcizet, Nat. Nanotechnol. **12**, 156 (2017).
[18] N. Rossi, F. R. Braakman, D. Cadeddu, D. Vasyukov, G. Tütüncüoglu, A. Morral, and M. Poggio, Nat. Nanotechnol. **12**, 150 (2017).
[19] T. Caniard, P. Verlot, T. Briant, P.-F. Cohadon, and A. Heidmann, Phys. Rev. Lett. **99**, 110801 (2007).
[20] O. Arcizet, P.-F. Cohadon, T. Briant, M. Pinard, and A. Heidmann, Nature (London) **444**, 71 (2006).
[21] See Supplemental Material at http://link.aps.org/supplemental/10.1103/PhysRevLett.122.083603 for details on theoretical calculations and experimental setup, which includes Refs. [22,23].
[22] D. Drouin, A. R. Couture, D. Joly, X. Tastet, V. Aimez, and R. Gauvin, Scanning **29**, 92 (2007).

[23] F. Zhou, A. L. Moore, J. Bolinsson, A. Persson, L. Fröberg, M. T. Pettes, H. Kong, L. Rabenberg, P. Caroff, D. A. Stewart *et al.*, Phys. Rev. B **83**, 205416 (2011).
[24] E. Gavartin, P. Verlot, and T. J. Kippenberg, Nat. Commun. **4**, 2860 (2013).
[25] A. Gloppe, P. Verlot, E. Dupont-Ferrier, A. Siria, P. Poncharal, G. Bachelier, P. Vincent, and O. Arcizet, Nat. Nanotechnol. **9**, 920 (2014).
[26] M. P. Mikhailova, *Handbook Series on Semiconductor Parameters* (World Scientific, Washington, DC, 1996), Vol. 1, p. 147.
[27] A. G. Every and A. K. McCurdy, *Second and Higher Order Elastic Constants*, edited by D. F. Nelson, Landolt-Börnstein - Group III Condensed Matter Vol. 29a (Springer, Berlin, Heidelberg, 1975), pp. 593–606, DOI: 10.1007/10046537_84.
[28] C. W. Helstrom, *Quantum Detection and Estimation Theory* (Academic Press, New York, 1976).
[29] R. L. Petry, Phys. Rev. **28**, 362 (1926).
[30] A. Xuereb, R. Schnabel, and K. Hammerer, Phys. Rev. Lett. **107**, 213604 (2011).